Available online at www.sciencedirect.com
SCIENCE DIRECT
Engineering Structures 28 (2006) 935–945
ENGINEERING STRUCTURES
www.elsevier.com/locate/engstruct

Seismic performance assessment of reinforced concrete bridge piers with lap splices

T.-H. Kim[a], B.-S. Kim[b], Y.-S. Chung[c], H.M. Shin[d,*]

[a] *Civil Engineering Research Team, Daewoo Institute of Construction Technology, 60 Songjuk-dong, Jangan-gu, Suwon, Kyonggi-do, 440-210, Republic of Korea*
[b] *Structure Research Department, Korea Institute of Construction Technology, 2311 Daewha-dong, Ilsan-gu, Goyang, Kyonggi-do, 411-712, Republic of Korea*
[c] *Department of Civil Engineering, Chung-Ang University, 72-1 Nae-ri, Daeduk-myun, Ansung, Kyonggi-do, 456-756, Republic of Korea*
[d] *Department of Civil and Environmental Engineering, Sungkyunkwan University, 300 Chunchun-dong, Jangan-gu, Suwon, Kyonggi-do, 440-746, Republic of Korea*

Received 15 June 2005; received in revised form 24 October 2005; accepted 26 October 2005
Available online 20 December 2005

Abstract

This study aims to analytically assess the seismic performance of reinforced concrete bridge piers with lap splices in longitudinal reinforcing bars, and to provide data for developing improved seismic design criteria. The accuracy and objectivity of the assessment process can be enhanced by using a sophisticated nonlinear finite element analysis program. A computer program, RCAHEST (Reinforced Concrete Analysis in Higher Evaluation System Technology), is used to analyze reinforced concrete structures. Models for material nonlinearity include tensile, compressive and shear models for cracked concrete and a model of reinforcing steel incorporating the smeared crack approach. A lap spliced bar element is newly developed to predict the inelastic behaviors of lap splices. The proposed numerical method for the seismic performance assessment of reinforced concrete bridge piers with lap splices is verified by comparing the analytical results with test data developed by the authors.

Keywords: Reinforced concrete bridge piers; Lap splices; Nonlinear finite element analysis program; Lap spliced bar element

1. Introduction

Recent earthquakes extensively damaged highway bridge structures. These structural failures revealed many structural deficiencies in bridges constructed before the new seismic design codes were established. In particular, reinforced concrete bridge piers with lap splices have contributed to the catastrophic collapse of many bridges. The poor detailing of the column lap spliced bars compounded the problem of seismic deficiency [1–3].

Lap splices in the plastic hinge zones, such as the base of the bridge piers, should not be used. However, the use of lap splice of longitudinal reinforcing bars at the base of bridge piers is sometimes practically unavoidable. These deficiencies result in a high potential for flexural strength degradation and ductility in the event of an earthquake. As a result of the damage that occurred to older bridges in recent earthquakes, major efforts are being directed towards developing and applying retrofit strategies to upgrade the seismic performance of older bridges [1–3].

The principal objective of this study is to provide basic knowledge on the seismic performance of reinforced concrete bridge piers with lap splices in the plastic hinge region. An evaluation method for determining the seismic performance of reinforced concrete bridge piers with lap splices is presented. This method uses a nonlinear finite element program (RCAHEST, Reinforced Concrete Analysis in Higher Evaluation System Technology), developed by the authors [4–8]. A lap spliced bar element is newly incorporated into the structural element library for RCAHEST to predict the seismic behavior of reinforced concrete bridge piers with lap splices of longitudinal reinforcing bars in the plastic hinge zone.

The lap spliced bar element is developed to consider the inelastic behavior by lap splices. The validity of existing equations [1] for calculating the maximum bar stress (or bond strength of lap splice) at failure along the splice length is examined. Then a simple model is used to provide reasonable

* Corresponding author. Tel.: +82 31 290 7513; fax: +82 31 290 7549.
E-mail address: hmshin@skku.ac.kr (H.M. Shin).

0141-0296/$ - see front matter © 2005 Elsevier Ltd. All rights reserved.
doi:10.1016/j.engstruct.2005.10.020

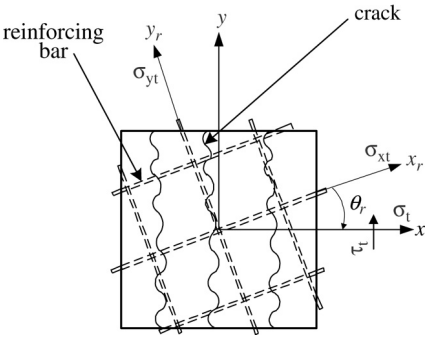

(a) Orientation of reinforcing bars and crack plane.

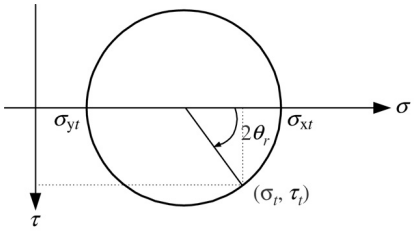

(b) Mohr circle representation of stress state in concrete.

Fig. 1. Tensile stress in concrete in the direction normal to the crack plane.

predictions of the seismic response of reinforced concrete bridge piers with inadequate length of lap splices at the column-to-foundation connection.

Experimental and analytical results show that even under low or moderate earthquake motions, bridge pier ductility significantly decreases because of bond failure in the lap splices of longitudinal reinforcing bars in the plastic hinge zone. Nonlinear analysis results for various reinforced concrete bridge piers with lap splices subjected to seismic loading agreed well with the test data developed by the authors. For the seismic performance assessment, the displacement ductility capacity is also computed for bridge piers with lap splices.

2. Nonlinear material model for reinforced concrete

The nonlinear material model for reinforced concrete is composed of the models for concrete and a model for the reinforcing bars. Models for concrete may be divided into models for uncracked concrete, which is isotropic, and for cracked concrete. For cracked concrete, three models representing the behavior of concrete in the direction normal to the crack plane, in the direction of the crack plane, and in shear direction at the crack plane, respectively, were adopted. The basic and widely-known model adopted for crack representation is based on the non-orthogonal fixed-crack method of the smeared crack concept. The approach using this model is practical for cyclic loading whose history needs to be recorded. This section summarizes the models used in this study, and more details are provided in references [5,6,8].

2.1. Model for uncracked concrete

The elasto-plastic and fracture model for the biaxial state of stress proposed by Maekawa and Okamura [9] is used as

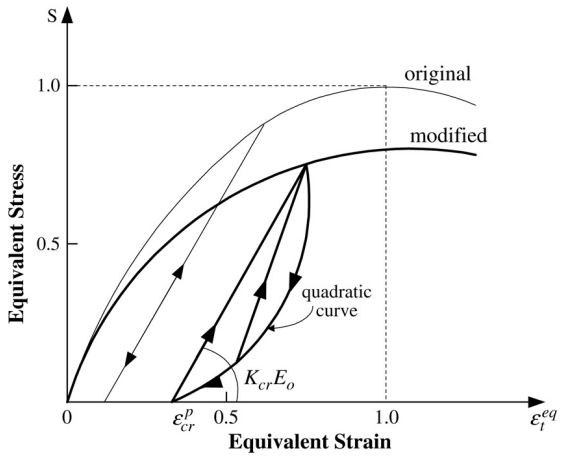

Fig. 2. Equivalent stress-equivalent strain relationship for concrete during unloading and reloading.

the constitutive equation for uncracked concrete. For uncracked concrete, the nonlinearity, anisotropy, and strain softening effects are expressed independent of the loading history.

2.2. Model for cracked concrete

The stress–strain relations are modeled by decomposing the stress and strain in directions parallel to, along, and normal to cracks, respectively. Thus, the constitutive law adopted for cracked concrete consists of tension stiffening, compression and shear transfer models.

A refined tension stiffening model is obtained by transforming the tensile stresses of concrete into a component normal to the crack. With this refined model, improved accuracy is expected, especially when the reinforcing ratios in the orthogonal directions are significantly different and when the reinforcing bars are distributed only in one direction (see Fig. 1). The model proposed by Shima et al. [10] is basically used as the tension stiffening model for unloading and reloading.

A modified elasto-plastic fracture model [11] is used to describe the compressive behavior of concrete struts in between cracks in the direction of the crack plane. The model modifies the fracture parameter in terms of the strain perpendicular to the crack plane to describe the degradation in compressive stiffness (see Fig. 2). Cyclic loading damages the inner concrete and energy is dissipated during the unloading and reloading processes.

The shear transfer model based on the contact surface density function [12] is used to consider the effect of shear stress transfer due to the aggregate interlock at the crack surface (see Fig. 3). The contact surface is assumed to respond elasto-plastically. The model is applicable to any arbitrary loading history. As the shear transfer model for unloading and reloading, the model modified by the authors [6] is used.

2.3. Model for the reinforcing bars in concrete

The stress acting on the reinforcing bar embedded in concrete is not uniform and becomes maximum at locations

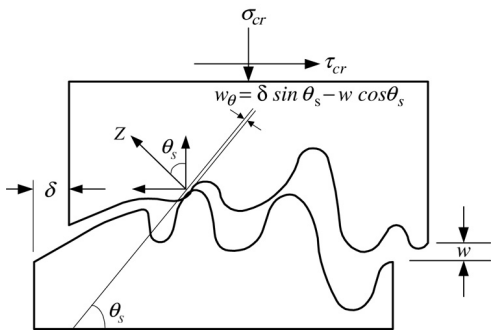

Fig. 3. Shear stress transfer through crack surface in concrete.

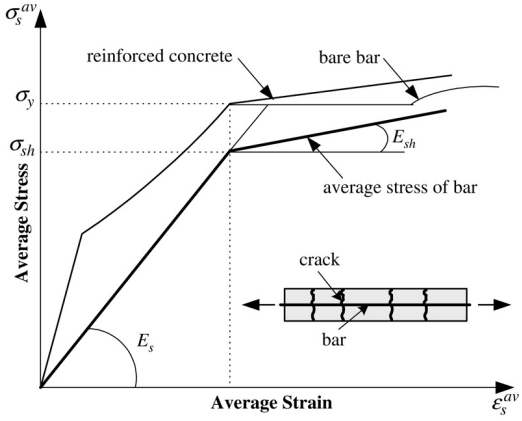

Fig. 4. Yield condition for reinforced concrete.

where the bar is exposed to a crack plane. The constitutive equations for the bare bar may be used if the stress–strain relation remains in the elastic range. The post-yield constitutive law for the reinforcing bar in concrete considers the bond characteristics, and the model is a bilinear model (see Fig. 4).

Kato's model [13] for the bare bar under reversed cyclic loading and the assumption of stress distribution described by a cosine curve were used to derive the mechanical behavior of reinforcing bars in concrete under reversed cyclic loading.

For reinforcing bars under extreme compression, the lateral bar buckling tends to occur, which greatly affects the post peak behavior and member ductility. To account for the buckling of reinforcing bars, the average stress–strain behavior after concrete crushing is assumed to be linearly decreasing until the 20% average steel stress is reached. This relation has been derived from a parametric study by using finite element analysis [8].

2.4. Models and assumptions for the interface

The local discontinuous deformation, which is a part of the anchorage slip, shear slip at the joint plane, and penetration at the joint plane, occurs according to the stiffness changing rapidly in the column and foundation etc. (see Fig. 5). The effects of local discontinuities are different according to the structural dimensions, and their effects on the load–displacement relations for the reinforced concrete bridge piers should be included in the analysis. Therefore, in order to

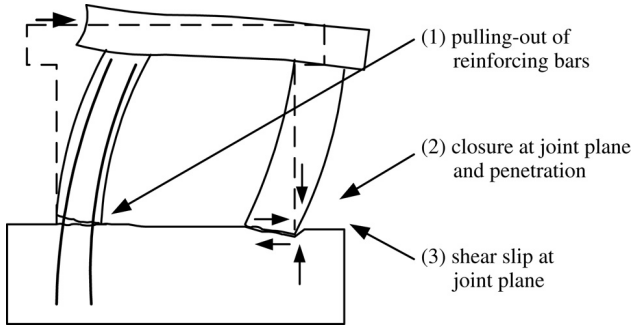

Fig. 5. Three types of localized discontinuous deformation at boundary plane.

predict the response of the structures at the boundary plane with accuracy, the interface element is required.

The interface model is based on the discrete crack concept. The strain–slip relation proposed by Shima et al. [10] is used as the analytical model for the pulling-out of reinforcing bars from the base caused by the tension in steel. The model for closure at the joint plane also considers the effect of the localized stress distribution. The shear slip model is derived from the Li and Maekawa model [12] of the reinforced concrete plane stress element.

2.5. Confinement in concrete by reinforcements

The transverse reinforcements confine the compressed concrete in the core region and inhibit the buckling of the longitudinal reinforcing bars. In addition, the reinforcements also improve the ductility capacity of the unconfined concrete.

This study adopted a model proposed by Mander et al. [14]. The models consider the yield strength, the distribution type, and the amount of the longitudinal and transverse reinforcing bars to compute the effective lateral confining stress and the ultimate compressive strength and strain of the confined concrete.

3. Model for the lap spliced bar

A reinforced concrete bridge pier with lap splices at its section of maximum moment can lose its lateral load resistance due to bond failure of the splice in the plastic hinge zone. The subsequent response is characterized by rapid strength degradation and very narrow energy dissipation loops. To accurately predict the global behavior of this type of bridge pier with inadequate splice at its base, two fundamental analytical tools are needed. The first is a nonlinear finite element analysis program that can be used to determine the stress transfer conditions in and around the lap spliced bars. The second is a bond stress–slip relationship describing the anchorage of the dowel bars in the reinforced concrete bridge pier.

3.1. General

The force-transfer mechanism in conventional lap splices is quite complex. However, the strength of the lap splices can be understood by considering the mechanism of failure.

The behavior of lap splices under cyclic loading is different from that for splices under monotonic loading or repeated unidirectional loading. Some of the earliest research work, relevant to splice behavior under repeated and reversed cyclic loading, was carried out by Fagundo et al. [15]. Their work centered mainly on the influence of load history and the effects of varying levels of confinement on the strength and ductility of lapped splices in the constant moment zone in beams. Paulay et al. [16] undertook a pilot experimental investigation of the behavior of lapped splices in the end region of reinforced concrete bridge piers and columns of a multistory frame under reversed cyclic loadings. Panahshahi et al. [17] studied the performance of compression lapped splices in column and beams under inelastic cyclic loading. Therefore, to define the characteristics needed in the design of retrofit methods for such splices under seismic loadings, quantitative information is needed on the specific influences of tangential and radial bar spacing and bar cover on lap splice performance.

3.2. Bond stress–slip relationships

Likely bar force-loaded end displacement relationships for a typical dowel were computed by using the bond stress–slip relationships reported by Hawkins and Lin [18]. For a bar force, F, less than yield, the loaded end displacement, S, can be computed approximately by the following expression:

$$S = \frac{F}{K} \tag{1}$$

where $K = (339.31d_b^2 + 332740.87)\sqrt{\frac{f_c'}{22.06}}$ (N/mm).

For a bar force, F, greater than the yield bar force, F_y, the loaded end displacement, S, is given by:

$$S = \frac{F_y}{K} + \frac{(F - F_y)}{K_s} \tag{2}$$

where $K = (339.31d_b^2 + 332740.87)\sqrt{\frac{f_c'}{22.06}}$ (N/mm); d_b = diameter of bar; f_c' = compressive strength of concrete; $K_s = K \cdot \frac{E_{sh}}{E_s}$; E_{sh} = strain hardening modulus of the bar; and E_s = modulus of elasticity of the bar.

For a bar subjected to high intensity reversed cyclic loading, the appropriate bond stress–slip relationship can be idealized as shown in Fig. 6 [19]. For monotonic loading to failure, the reduction factor γ is unity and $\tau_{b,\max}$, τ_y, S_0, and S_y are given by the following expressions.

$$\tau_{b,\max} = \left(\frac{f_c' - 15.86}{2.07}\right)^{\frac{2}{3}} \times 6.89 \le 34.47 \text{ MPa} \tag{3}$$

$$\tau_y = 0.1\, f_c' \text{ or } 2.76 \text{ MPa, whichever is smaller} \tag{4}$$

$$S_0 = 0.03089\left(\frac{f_c'}{d_b}\right)^{\frac{1}{3}} + \frac{12.26}{f_c' d_b} \tag{5}$$

$$S_y = 0.5 \times \text{ lug spacing} \tag{6}$$

where $\tau_{b,\max}$ = maximum bond stress; τ_y = bond stress at bar yield; S_0 = slip at maximum bond stress; and S_y = slip at bar yield.

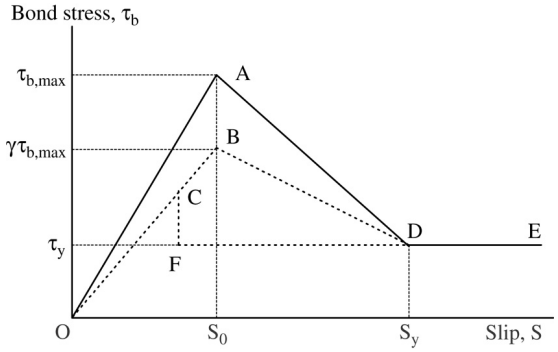

Fig. 6. Idealized bond stress–slip relationship [19].

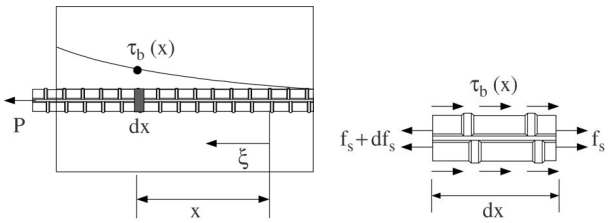

(a) Specimen. (b) Free body diagram of a bar element.

Fig. 7. Diagrams for the derivation of equilibrium equation.

Under stress reversals at which the bar behaves inelastically both in tension and compression, a lower bound to the bond stress–slip relationship is represented by broken lines OBDE and OCFE in Fig. 6. Relationship OBDE is the response for a non-yielding bar, and OCFE is the response for a bar that starts to yield at C. The maximum bond stress, $\tau_{b,\max}$, that can be developed, is a function of the intensity of the reversed loading, and the range of that loading.

The relationship between bar force and loaded end displacement can be determined as shown in Fig. 7(a). A force, P, is applied to the attack end of a bar, and bond stresses are created along the embedded length of the bar. Fig. 7(b) shows a free body diagram of a typical bar element of length dx. Bond stresses are assumed to be uniformly distributed over the surface of this element. Axial equilibrium gives:

$$\tau_b = \frac{A_b}{\pi d_b}\frac{df_s}{dx} \tag{7}$$

where τ_b = bond stress; f_s = steel stress; and A_b = bar cross-sectional area.

The bond stress, τ_b, is dependent on the local slip, S, and this relationship can be formulated as:

$$\tau_b = f(S) = k_1 S \qquad \text{for } S \le S_0 \tag{8}$$

and

$$\tau_b = f(S) = 2.76 \text{ MPa} \qquad \text{for } S > S_0 \text{ or } S \text{ for bar yield} \tag{9}$$

where $S = \int_0^x \varepsilon(\xi)\mathrm{d}\xi$.

The force P is computed as:

$$P = \int_0^x \tau_b \pi d_b \mathrm{d}\xi. \tag{10}$$

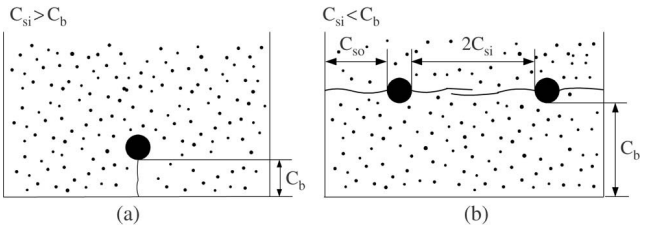

Fig. 8. Bond cracks and notations for Eq. (11).

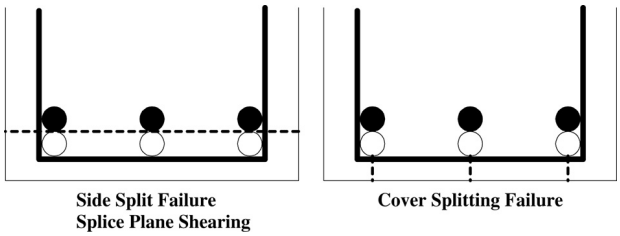

Fig. 9. Splice failure modes covered by Eq. (11).

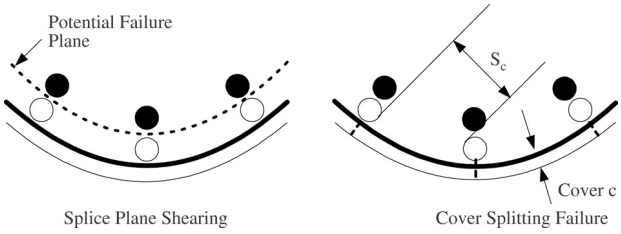

Fig. 10. Splice failure possible for circular columns.

By substituting τ_b into Eq. (10), a set of linear second-order differential equations can be obtained. The bond stress distribution, the steel stress distribution, and the load–displacement relationship at the attack end of the bar can be determined by solving these differential equations.

3.3. Lap splice capacity

Lap splice failure can occur in two ways: a splitting crack can develop along the length of the outermost bar and cause it to fail in bond, or cracks can propagate between the lap spliced bars and cause a loss of load transfer between them. The failure mode depends on the details of the variables in the cross-section [1].

A detailed study of bond failure was performed by Darwin et al. [20]. The following equation was used to calculate the maximum force at bond failure of a spliced bar in a member with a rectangular cross section subjected to monotonic loading to failure.

$$\frac{T_b}{(f'_c)^{\frac{1}{4}}} = [1.507 l_d(c_m + 0.5d_b) + 50.96A_b]\left(0.1\frac{c_M}{c_m} + 0.9\right) + 53.26 t_r t_d \frac{N_{tr}A_{tr}}{n_b} + 1019 \quad (11)$$

where T_b = maximum force for bond failure; l_d = splice length (mm); c_M, (c_m) = maximum (minimum) value of c_s or c_b, ($c_M/c_m \le 3.5$) (mm); c_s = minimum of ($c_{si} + 6.35$ mm, c_{so}) or minimum of (c_{si}, c_{so}) (mm); c_{si} = one-half of clear spacing between spliced bars (mm); c_b = bottom cover for spliced bars (mm); c_{so} = side cover of reinforcing bars (mm); N_{tr} = number of transverse reinforcing bars (stirrups or ties) crossing l_d; A_{tr} = area of each stirrup or tie crossing the potential plane of splitting (mm^2); n_b = number of longitudinal bars being spliced along the plane of the split (smaller of c_b or c_s); $t_t = 9.6R_r + 0.28$; $t_d = 0.72(d_b/25.4) + 0.28$; and R_r = relative rib area (0.065 to 0.14). The notation for c_{si}, c_b, and c_{so} is shown in Fig. 8. Values used in Eq. (11) depend on the mode of bond failure.

Eq. (11) clearly covers, as shown in Fig. 9, both the possibility of a splice plane shearing failure mode and a cover splitting failure mode. To adapt Eq. (11) to the circular columns, it is necessary to modify the c_{si}, c_m, c_M, and c_b terms in a manner consistent with the properties of those specimens. Fig. 10 shows the splice plane shearing and cover splitting failure modes for the circular columns, which are analogous to the same modes for a rectangular beam. Clearly, the critical dimensions relate to the properties of the column bars (open circles) and not the properties of the dowel bars (shaded circles). The following transformations apply:

$$c_m = c \quad \text{and} \quad c_M = 0.5S_c + 6.35 \text{ mm} \quad (12)$$

where c = cover over extreme tension bar (mm); and S_c = clear spacing in circumferential direction between columns bars (mm).

The maximum bond stress that can be developed by the column bars reduces once the peak reversing stress exceeds 75% of the maximum stress for bond failure under monotonic loading. Based on the information presented by Hawkins et al. [19], for test columns, the reduction factor γ on the maximum stress is taken as

$$\gamma = 0.9 - 5(S - 0.75S_0) \ge 0.65 \quad \text{for } \tau_b > 0.75\tau_{b,\max}. \quad (13)$$

The term $5(S - 0.75S_0)$ does not start to apply until S exceeds $0.75S_0$ for both positive and negative loading.

4. Nonlinear finite element analysis program (RCAHEST)

RCAHEST is a nonlinear finite element analysis program for analyzing reinforced concrete structures. The program was developed by Kim and Shin [4], at the Department of Civil and Environmental Engineering, Sungkyunkwan University. The program is used to model various reinforced concrete structures under a variety of loading conditions.

4.1. General features of RCAHEST

The proposed structural element library RCAHEST (Reinforced Concrete Analysis in Higher Evaluation System Technology) is built around the finite element analysis program shell named FEAP, developed by Taylor [21]. FEAP is characterized by a modular architecture and has features which allow custom elements, input utilities, and custom strategies and procedures to be easily introduced.

The elements developed for the nonlinear finite element analyses of reinforced concrete bridge piers under earthquake

Table 1
Properties of reinforced concrete column specimens

Specimen[a]		FS-H-LS000	FS-H-LS050	FS-H-LS100	NS-HT2-H-L2	NS-HT2-A-L2	NS-HT4-H-L2	NS-HT4-A-L2
Diameter of cross section (mm)			1200			1200		
Effective height (mm)			3200			4800		
Aspect ratio			2.67			4.00		
Longitudinal reinforcement	Material		SD30A D25			SD30A D19		
	Yielding stress (MPa)		331.3			343.2		
	Reinforcement ratio (%)		1.60			1.01		
Transverse reinforcement	Material		SD30A D13			SD30A D10		
	Yielding stress (MPa)		326.2			372.7		
	Volumetric ratio (%)		0.340			0.127		
Strength of concrete (MPa)			24.5			24.8		
Lap spliced length (mm)			600			600		
Lap spliced ratio (%)		0	50	100	50	100	50	100

[a] FS Series [23]; NS Series [22].

are the reinforced concrete plane stress element and the interface element [4–8]. A lap spliced bar element is newly incorporated into the structural element library for RCAHEST to predict the inelastic behavior of reinforced concrete bridge piers with lap splices of longitudinal reinforcing bars in the plastic hinge zone. The material models described in the previous sections are used as the stress–strain relations at gauss integration points of each element.

4.2. Formulation for lap spliced bar element

The lap spliced bar element was developed for the inelastic finite element analyses of reinforced concrete bridge piers with lap splices subjected to seismic loading. The stress and strain of the lap spliced bar can be obtained by using a truss element that is modeled as an independent element. The elements are formulated by coordinate transformation from the element coordinate system to the reference coordinate system.

The strain of a lap spliced bar is given by:

$$\varepsilon = \varepsilon_s + \varepsilon_{\text{slip}} \tag{14}$$

where ε_s= strain of bar; and $\varepsilon_{\text{slip}} = 2 \times \text{slip}/l_d$.

The stress–strain relationship of a lap spliced bar can be formulated as:

$$\{\sigma_s\} = [D]\{\varepsilon_s\} = [D]\{\varepsilon - \varepsilon_{\text{slip}}\} \tag{15}$$

where $\{\sigma_s\}$ = stress of bar; and $[D]$ = modulus of elasticity of the bar.

5. Numerical examples

The data for the reinforced concrete bridge piers with lap splices tested by the authors [22,23] are used to verify the applicability of the lap spliced bar element.

5.1. Description of test specimens

In the experimental testing of structures to assess performance and available ductility of the structures during severe earthquakes, the appropriate displacement history to be imposed for simulation of seismic loading must be determined.

The full-scale test specimens of reinforced concrete bridge piers were designed in conformity to the provisions of KRBD (Korea Roadway Bridge Design) code [24], which has not adopted the seismic design concept. The earlier code is used for designs to investigate the seismic performances of existing reinforced concrete bridge piers constructed before the seismic design concept was adopted in the design code in Korea. The mechanical properties of the specimens are listed in Table 1 and the geometric details are shown in Figs. 11 through 13. All reinforced concrete column specimens were tested under $0.07 f_c' A_g$ of constant compressive axial load as shown in Fig. 14 to simulate the gravity load from bridge superstructures.

Quasi-static cyclic load tests were carried out under displacement control. Fig. 15 shows the cyclic load history, which was based on the lateral displacement pattern of increasing magnitude of yield displacement. More detailed descriptions of both schemes are available in references [22, 23].

5.2. Description of analytical model

Fig. 16 shows the finite element discretization and the boundary conditions for nonlinear analyses of the reinforced concrete column specimens. Fig. 17 shows a method for transforming a circular section into rectangular strips for the purpose of using plane stress elements. For rectangular sections, equivalent strips are calculated. After the internal forces are calculated, the equilibrium is checked. Loading cycles with displacement control are applied as this allows the analysis beyond the ultimate load where the load at the maximum strain is recognized from the load–displacement curve.

5.3. Comparison with experimental results

FS series and NS series were the specimen names, and the respective load–displacement relationships for the specimens

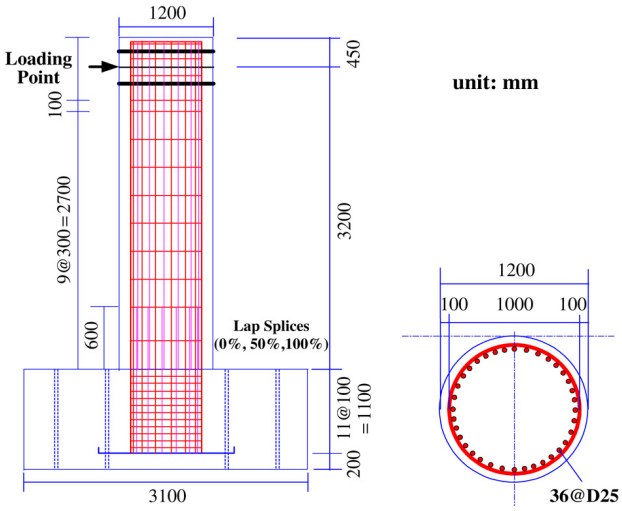

(a) Elevation. (b) Cross-section.

Fig. 11. Details of FS series specimen.

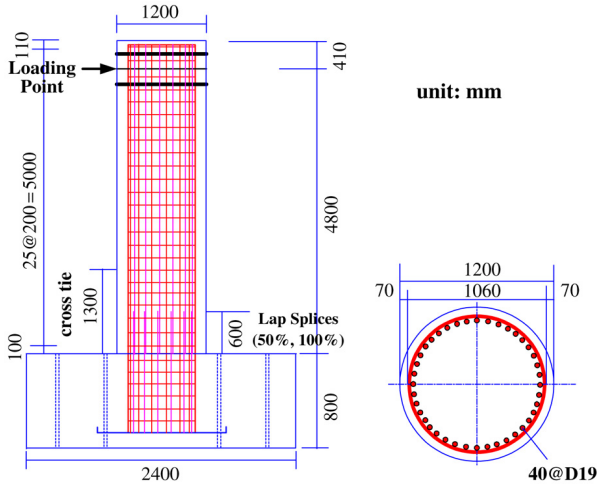

(a) Elevation. (b) Cross-section.

Fig. 12. Details of NS series specimen.

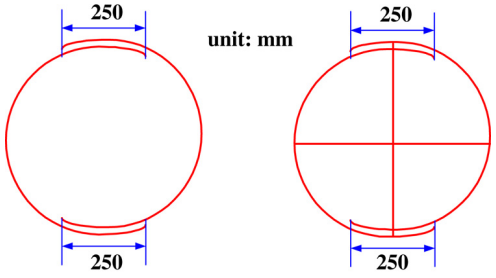

Fig. 13. Details of NS series tie: (a) HT2; and (b) HT4.

are shown in Figs. 18 and 19. The value given by all specimens were similar with the analytical results; comparative data are summarized in Table 2. Analytical results show reasonable correspondence with the experimental results.

All the results support that the failure mode and ductility level of reinforced concrete bridge piers with lap splices after yielding of longitudinal reinforcement can be estimated by the

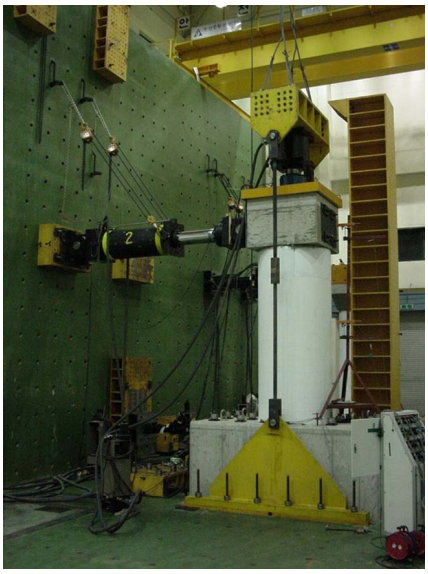

(a) FS series.

(b) NS series.

Fig. 14. Loading setup.

finite element analysis proposed in this paper. The proposed model provides a good prediction of the maximum loads for all specimens; also, the model provides a conservative prediction of the deflections at the given loads for all specimens failing in bond.

The hysteresis curves show that the strength reduction is largely due to the degradation of the splice region at the bottom of the column. The failure modes are brittle because of rapid strength deterioration directly following debonding of longitudinal steels. The test specimen without lap splices developed more ductile hysteresis loops than those specimens with lap splices. This occurs due to a slip of the longitudinal bars in the spliced region shortly after yielding in the reinforcement.

Seismic performance of reinforced concrete bridge piers can be evaluated as displacement ductility. The ductility of reinforced concrete bridge piers is associated with shear and flexural carrying capacities. The ductility of reinforced concrete bridge piers with lap splices after the yielding of longitudinal

Table 2
Experiment and analysis results

Specimen[a]	Experiment				Analysis				Ratio of experimental and analytical results			
	V_{max} (kN)	δ_y (mm)	δ_u (mm)	μ	V_{max} (kN)	δ_y (mm)	δ_u (mm)	μ	V_{max}	δ_y	δ_u	μ
FS-H-LS000	1240.8	16.5	58.0	3.5	1085.8	17.7	45.0	2.5	1.14	0.93	1.29	1.40
FS-H-LS050	1096.8	13.5	40.0	3.0	985.0	15.0	32.0	2.1	1.11	0.90	1.25	1.43
FS-H-LS100	978.4	8.6	21.8	2.5	873.9	13.0	21.0	1.6	1.12	0.66	1.04	1.56
NS-HT2-H-L2	721.2	32.1	84.6	2.6	576.2	26.0	84.0	3.2	1.25	1.23	1.01	0.81
NS-HT2-A-L2	641.4	29.6	59.0	2.0	548.3	22.0	42.0	1.9	1.17	1.35	1.40	1.05
NS-HT4-H-L2	664.7	33.2	98.5	3.0	574.9	28.0	88.0	3.1	1.16	1.19	1.12	0.97
NS-HT4-A-L2	575.7	30.5	59.2	1.9	553.9	26.0	48.0	1.8	1.04	1.17	1.23	1.06
Total						Mean			1.14	1.06	1.19	1.18
						Standard deviation			0.06	0.24	0.14	0.28

[a] FS Series [23]; NS Series [22].

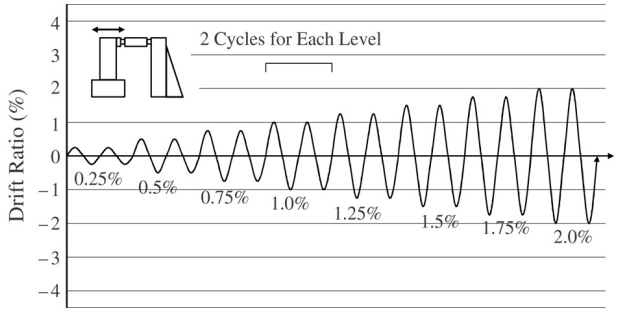

(a) FS series.

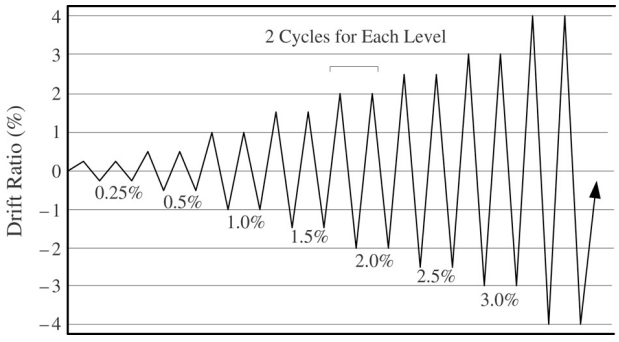

(b) NS series.

Fig. 15. Loading history for test.

reinforcement may also be simulated by computation using finite elements. Seven experimental results were compared with the finite element analytical results. In predicting the results of the FS series and NS series involving primary bond failures, under a variety of reinforcement and loading conditions, the mean ratios of experimental-to-analytical ductility capacities were 1.18 at a standard deviation of 28%. From comparisons of the measured load–deflection responses with predicted responses, it is apparent that the ductility of the specimens can be limited by the crushing of the concrete equally as well as by bond failure of the lap splices. Both the experimental and analytical results show that the increase of the lap spliced ratio in reinforced concrete bridge piers yields lower ductility. Displacement ductility ratios significantly reduced for specimens with lap splices of longitudinal steels.

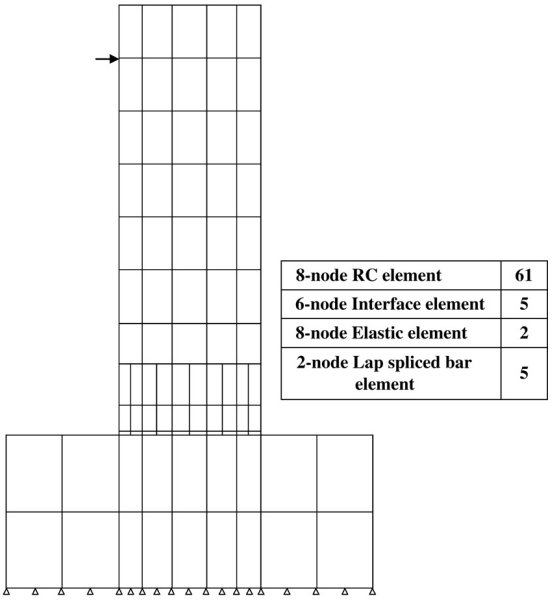

Fig. 16. Finite element mesh for reinforced concrete column specimen.

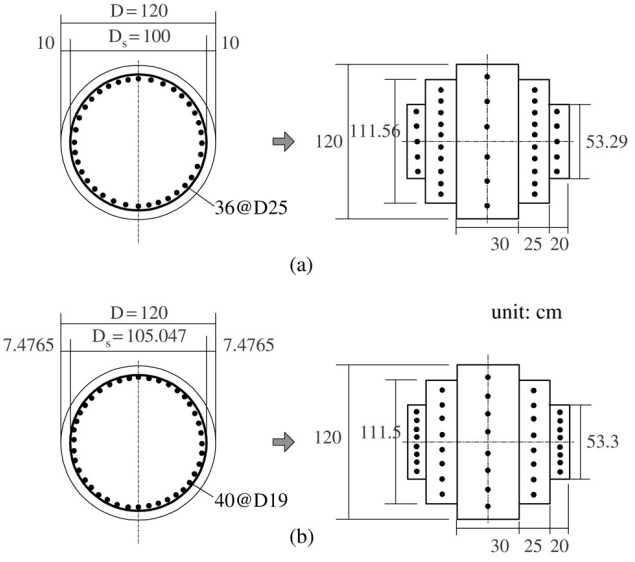

Fig. 17. Transformation of a circular column to an idealized equivalent rectangular column: (a) FS series; and (b) NS series.

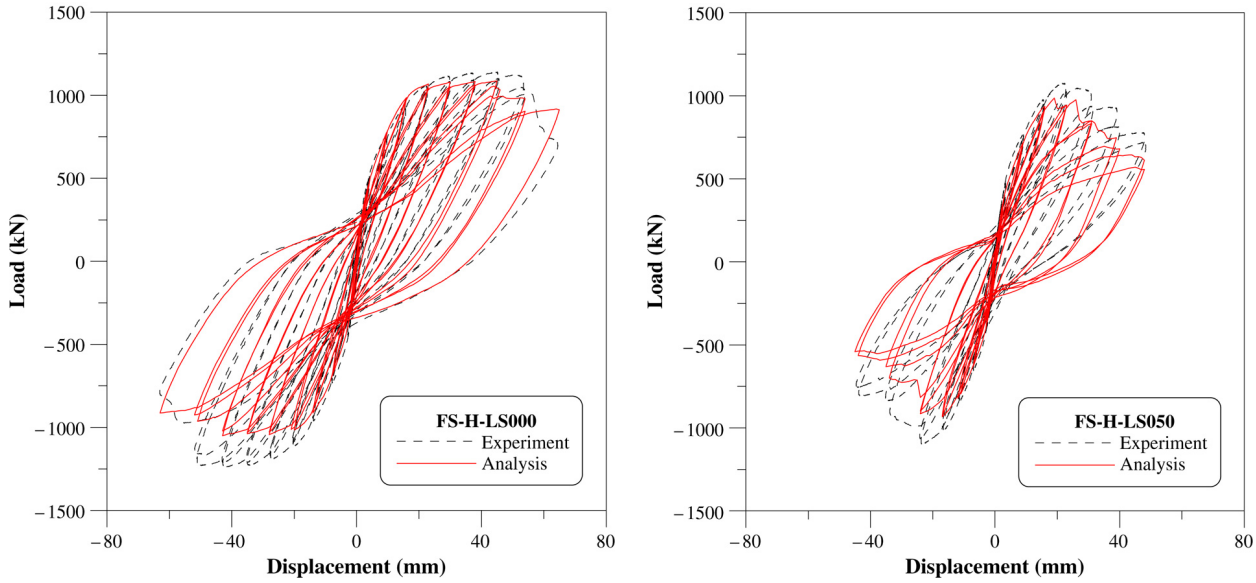

(a) FS-H-LS000.

(b) FS-H-LS050.

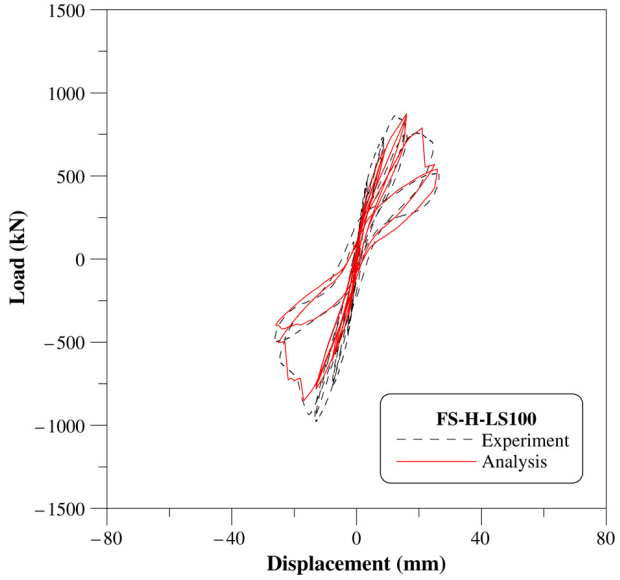

(c) FS-H-LS100.

Fig. 18. Load–displacement curve.

Of all the parameters that influence the strength and the energy dissipation ability of lap splices, the amount and distribution of confining steel is probably the most important one, particularly in the case of structures required to withstand earthquake induced forces. By controlling the formation of cracks and their subsequent propagation, transverse bars greatly enhance lap strength and particularly ductility. The amount and distribution of transverse reinforcement is of importance in the detailing of lap splices. The use of continuous reinforcement in the plastic hinge zone moderately improves the lateral displacement hysteresis loop. The structural degradation is likely to be delayed. The lap splice of longitudinal steels in the potential plastic hinge zone of reinforced concrete bridge piers should be prevented even in a moderate seismic region, unless pertinent transverse confinement can be established.

6. Summary and conclusions

A method for analyzing the nonlinear hysteretic behavior and ductility capacity of reinforced concrete bridge piers with lap splices under earthquakes was proposed. Theory and formulations for analytical models to be implemented with numerical methods for predicting the behavior of reinforced concrete bridge piers with lap splices subjected to seismic loading were described. Analytical results by the proposed method were in reasonable agreement with experimental data. The proposed method also predicted the load capacities, failure

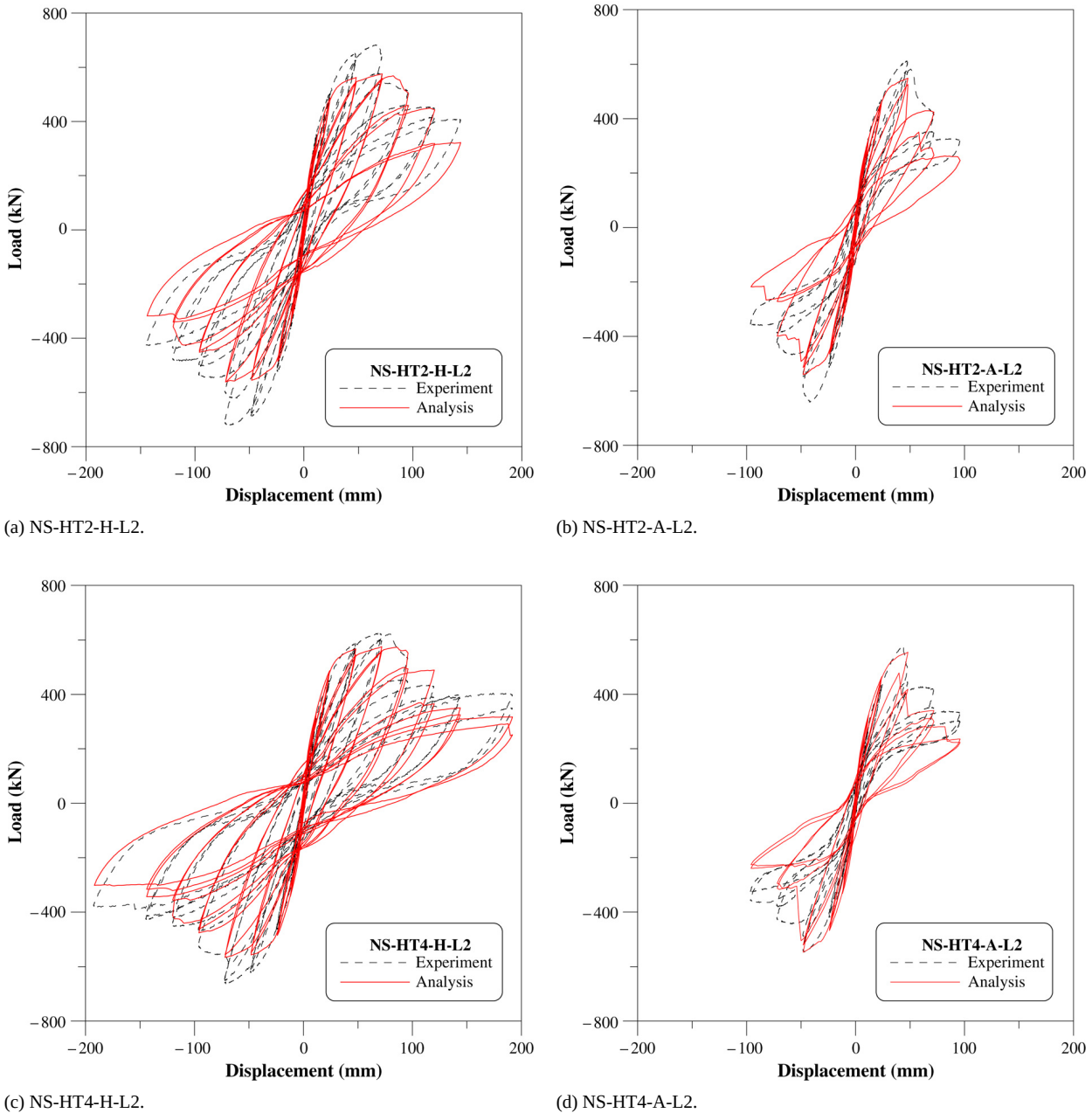

(a) NS-HT2-H-L2.

(b) NS-HT2-A-L2.

(c) NS-HT4-H-L2.

(d) NS-HT4-A-L2.

Fig. 19. Load–displacement curve.

modes, and load–deformation responses of reinforced concrete bridge piers with acceptable accuracy.

Based on the results of the numerical simulations and comparisons with experimental data, the following conclusions were reached.

1. The proposed constitutive model and numerical analysis describe the inelastic behavior of the reinforced concrete bridge piers with lap splices under earthquakes with acceptable accuracy. This method may be used for the seismic analysis and design of reinforced concrete bridge piers.

2. Experimental and analytical values for yield and ultimate displacements and ductility capacity of the reinforced concrete bridge piers with lap splices show reasonable agreement.

3. Non-seismically designed reinforced concrete bridge piers with lap splicing of longitudinal reinforcement in the plastic hinge zone typically failed at low ductility levels. This was due to the debonding of the lap splice, which resulted from insufficient development length of the longitudinal bars. It is not desirable to permit the lap splice of longitudinal steels in the potential plastic hinge zone without increasing the transverse confinement, in a moderate seismic region.

4. Nonlinear finite element analysis may be used to investigate the design details and the load–deflection response of reinforced concrete bridge piers with lap splices. Also, failure modes and ductility may be checked for seismic resistant design.

5. More effort should be directed to include certain procedures in the current design codes so that engineers can work toward an acceptable method for evaluating the available strength in existing reinforced concrete bridge piers with lap splices.

Acknowledgements

The study described in this paper was supported by the Ministry of Construction and Transportation through the Korea Bridge Design and Engineering Research Center. The authors wish to express their gratitude for the support received.

References

[1] Lin Y. Seismic behavior of bridge pier column lap splices. Ph.D. thesis, Department of Civil Engineering, University of Illinois at Urbana-Champaign; 1996.
[2] Jaradat OA, McLean DI, Marsh ML. Performance of existing bridge columns under cyclic loading — part 1: experimental results and observed behavior. ACI Structural Journal 1998;95(5):695–704.
[3] Aboutaha RS, Engelhardt MD, Jirsa JO, Kreger ME. Experimental investigation of seismic repair of lap splice failures in damaged concrete columns. ACI Structural Journal 1999;96(2):297–306.
[4] Kim T-H, Shin HM. Analytical approach to evaluate the inelastic behaviors of reinforced concrete structures under seismic loads. Journal of the Earthquake Engineering Society of Korea EESK 2001;5(2):113–24.
[5] Kim T-H, Lee K-M, Shin HM. Nonlinear analysis of reinforced concrete shells using layered elements with drilling degree of freedom. ACI Structural Journal 2002;99(4):418–26.
[6] Kim T-H, Lee K-M, Yoon C-Y, Shin HM. Inelastic behavior and ductility capacity of reinforced concrete bridge piers under earthquake. I: theory and formulation. Journal of Structural Engineering ASCE 2003;129(9): 1199–207.
[7] Kim T-H, Lee K-M, Yoon C-Y, Shin HM. Inelastic behavior and ductility capacity of reinforced concrete bridge piers under earthquake. II: numerical validation. Journal of Structural Engineering ASCE 2003; 129(9):1208–19.
[8] Kim T-H, Lee K-M, Chung Y-S, Shin HM. Seismic damage assessment of reinforced concrete bridge columns. Engineering Structures 2005;27(4): 576–92.
[9] Maekawa K, Okamura H. The deformational behavior and constitutive equation of concrete using elasto-plastic and fracture model. Journal of the Faculty of Engineering, University of Tokyo (B) 1983;37(2):253–328.
[10] Shima H, Chou L, Okamura H. Micro and macro models for bond behavior in reinforced concrete. Journal of the Faculty of Engineering, University of Tokyo (B) 1987;39(2):133–94.
[11] Okamura H, Maekawa K, Izumo J. RC plate element subjected to cyclic loading. IABSE Colloquium Delft 1987;54:575–90.
[12] Li B, Maekawa K, Okamura H. Contact density model for stress transfer across cracks in concrete. Journal of the Faculty of Engineering, University of Tokyo (B) 1989;40(1):9–52.
[13] Kato B. Mechanical properties of steel under load cycles idealizing seismic action. CEB Bulletin D'Information 1979;131:7–27.
[14] Mander JB, Priestley MJN, Park R. Theoretical stress–strain model for confined concrete. Journal of Structural Engineering ASCE 1988;114(8): 1804–26.
[15] Fagundo F, Gergely P, White RN. The behaviors of lapped splices in R/C beams subjected to repeated loads. Report no 79-7. Ithaca: Department of Structural Engineering, Cornell University; 1979.
[16] Paulay T, Zanza TM, Scarpas A. Lapped splices in bridge piers and in columns of earthquake resisting reinforced concrete frames. Research report 81-6. Christchurch (New Zealand): Department of Civil Engineering, University of Canterbury; 1981.
[17] Panahshahi N, White RN, Gergely P. Compression and tension lap splices in reinforced concrete members subjected to inelastic cyclic loading. Report no 87-2. Ithaca: Department of Structural Engineering, Cornell University; 1987.
[18] Hawkins NM, Lin I. Bond characteristics of reinforcing bars for seismic loadings. In: Proceedings, third Canadian conference on earthquake engineering. vol. 2. 1979, p. 1225–34.
[19] Hawkins NM, Lin I, Ueda T. Anchorage of reinforcing bars for seismic forces. ACI Structural Journal 1987;84(5):407–18.
[20] Darwin D, Tholen ML, Idun EK, Zuo J. Splice strength of high relative rib area reinforcing bars. ACI Structural Journal 1996;93(1):95–107.
[21] Taylor RL. FEAP — A finite element analysis program, version 7.2 users manual, vols. 1–2. 2000.
[22] Lee DH, Park JY, Chung YS, Cho DY, Lee JH. Seismic performance evaluation of circular RC bridge piers with longitudinal steel lap splice. Proceedings of EESK Conference 2001;5(2):187–93 [in Korean].
[23] Kwahk IJ, Cho CB, Cho JR, Kim YJ, Kim BS. Quasi static test of lap spliced shear-flexure RC piers using real scale models. Proceedings of EESK Conference 2002;6(1):203–10 [in Korean].
[24] Ministry of Construction and Transportation. Korea roadway bridge design code. 1983.